4146 Vol. 40, No. 17 / September 1 2015 / Optics Letters Letter

Optics Letters

Defocus noise suppression with combined frame difference and connected component methods in optical scanning holography

HAIYAN OU,[1,*] HUIYU PAN,[1] EDMUND Y. LAM,[2] AND BING-ZHONG WANG[1]

[1]Institute of Applied Physics, University of Electronic Science and Technology of China, 610054 Chengdu, China
[2]Department of Electrical and Electronic Engineering, The University of Hong Kong, Pokfulam, Hong Kong, China
*Corresponding author: ouhaiyan@uestc.edu.cn

Received 19 June 2015; revised 29 July 2015; accepted 9 August 2015; posted 11 August 2015 (Doc. ID 243409); published 31 August 2015

Random phase masks can transform the defocus noise into a speckle-like pattern in optical scanning holography (OSH). In this Letter, we presented a speckle reduction based on combined frame difference and connected component method in a random phase-coded OSH system. The image quality of the reconstructed sections is improved with better visibility.

OCIS codes: (090.1995) Digital holography; (100.3190) Inverse problems; (100.3010) Image reconstruction techniques; (110.1758) Computational imaging.

http://dx.doi.org/10.1364/OL.40.004146

Optical scanning holography (OSH), as one of the digital holography techniques, has found wide applications such as microscopy [1,2], remote sensing [3,4], and image encryption, etc. [5,6]. In an OSH system, the combined coherence beams from two pupils are used for a two-dimensional (2D) heterodyne scan. The generated complex hologram contains three-dimensional (3D) volume information of the object [7].

To reconstruct an individual 2D section from the hologram, one can compute the convolution of the acquired hologram with the conjugate of the Fresnel zone plate (FZP) at the focused depth. This traditional method suffers from large undesired residual signals from other sections, i.e., defocus noise. To eliminate the defocus noise, methods, such as inverse imaging [8,9], Wigner filter [10], and Wigner distribution [11] have been proposed. Other methods based on acquiring two sets of measurements of the hologram have further improved the depth resolution, such as ways of using a dual-wavelength laser [12], double-location detection [13], and reconfigurable pupil [14].

Zhou found another way to deal with this problem, in which a random phase pupil was utilized to transfer the defocus noise into speckle-like patterns [15]. This kind of defocus noise is also a problem for optical image encryption where random phase mask is commonly used [5,16]. To reduce the defocus noise, one needs to calculate the average of the reconstructed section several times, which is quite time-consuming and cannot meet the requirements for real-time processing systems, such as *in vivo* holographic imaging.

In this Letter, we present for the first time to the best of our knowledge, a speckle-like defocus noise reduction method based on a frame difference and connected component (FDCC) method in a random phase encoded OSH system. Our results justify that the FDCC method can be an effective tool for sectional image despeckling in OSH.

The system setup for OSH is shown in Fig. 1. Two pupils located in front of the focal plane of lenses L_1 and L_2 are illuminated by two different beams from beam splitter (BS1), with frequencies centered at ω_0 and $\omega_0 + \Omega$, respectively. The combined beam is then used to scan the object, which is located a distance z away from the scanning mirror. The transmitted light from the object would be collected by lens 3 and sent to the photodiode (PD) for further electrical processing. The generated hologram can be expressed as

$$g(x, y) = \sum_{i=1}^{n} F^{-1}\{F\{I(x, y; z_i)\} \cdot \mathrm{OTF}(k_x, k_y; z_i)\}, \quad (1)$$

where $F[.]$ and $F^{-1}[.]$ represent Fourier transform and its inverse, x, y, are the space coordinates. z_i and $I(x, y, z_i)$ represent the depth location and the intensity distribution of

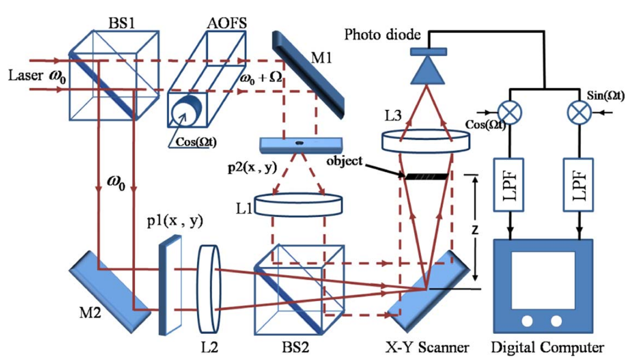

Fig. 1. Schematic of optical scanning holography. BS, beam splitter; M, mirror; AOFS, acousto-optic frequency shifter; LPF, low-pass filter. $p_1(x, y)$, $p_2(x, y)$ are pupils.

the i-th section, and $\mathrm{OTF}(k_x, k_y; z_i)$ is the optical transfer function of the system.

If we set the two pupils as $p_1(x,y) = \exp j[2\pi r(x,y)]$ and $p_2(x,y) = 1$, where $r(x,y)$ is a function of random numbers chosen from a uniform distribution between (0,1), then the OTF could be expressed as [7]

$$\mathrm{OTF}(k_x, k_y; z_i) = \exp\left[-j\frac{z_i}{2k_0}(k_x^2 + k_y^2)\right] \times P_1^*\left(-\frac{z_i k_x}{f}, -\frac{z_i k_y}{f}\right), \quad (2)$$

where k_0 is the wave number of the laser, k_x and k_y denote the spatial frequency, and f is the focal length of the lens. P_1 is the Fourier transform of p_1.

To reconstruct the j-th section, we choose the decoding pupils as p_{1d} and p_{2d}, where $p_{1d}(x,y) = 1$ and $p_1^*(-x,-y)p_{2d}(x,y) = 1$. The reconstructed distance is z_j in this case. The output thus becomes

$$I_{\mathrm{out}}(x,y) = F^{-1}\left[F[g(x,y)] \cdot \exp\left[j\frac{z_j}{2k_0}(k_x^2 + k_y^2)\right] \times P_{2d}\left(\frac{z_j k_x}{f}, \frac{z_j k_y}{f}\right)\right] = I(x,y;z_j) + N(x,y;z_j), \quad (3)$$

where $I(x,y;z_j)$ is the recovered section at z_j, while $N(x,y;z_j)$ is the speckle-like noise expressed as [15]

$$N(x,y;z_j) = \sum_{i\neq j} F^{-1}\left\{F\{I(x,y;z_i)\} \times \exp\left[j\frac{z_j - z_i}{2k_0}(k_x^2 + k_y^2)\right] \times P_1^*\left(-\frac{z_i k_x}{f}, -\frac{z_i k_y}{f}\right) \times P_{2d}\left(\frac{z_j k_x}{f}, \frac{z_j k_y}{f}\right)\right\}. \quad (4)$$

As mentioned above, this speckle-like haze needs to be suppressed for a better sectioning effect. One can reduce the noise by averaging multiple sectional images. However, the result is not so encouraging, even when averaging as many as 10 frames. Here, we propose the FDCC method to solve this problem.

The frame difference (FD) method is widely used in moving object detection from video sequences in which the changed part between different images is extracted to distinguish the moving objects and the background [17,18]. In our proposed method, FD is used to distinguish the reconstructed image and the speckle-like defocus noise. As this defocus noise is generated by independent random phase masks, the speckle-like pattern should be independent, and different as well. With different sectional images generated by an independent phase mask, the FD method is likely to have a good denoising effect, leaving a small portion of noise on the reconstructed image. The connected component (CC) labeling can then be applied to further delete the noise based on binary image analysis. CC labeling is a fundamental process for pattern recognition, computer vision, and image analysis [19,20]. It enable us to differentiate different objects based on features, such as area, perimeter, circularity ratio, and contour. In the random phase coded OSH system, the defocus noise shows a speckle-like pattern, which is not the case for the object. CC labeling is thus adapted to differentiate the object with the speckle-like noise based on the feature of area.

With the FD method, we can distinguish the object with different speckle-like noise, and CC labeling is then applied to eliminate the noise further. By combining these two methods, we expect to have a better sectioning effect in the random phase encoded OSH system.

The flow chart of the FDCC method is shown in Fig. 2. The steps of the proposed algorithm are as follows.

(1) Generate two holograms, $g_1(x,y)$ and $g_2(x,y)$, with different random phase masks.
(2) Get the reconstructed j-th section, $I_1(x,y;z_j)$ and $I_2(x,y;z_j)$, respectively.
(3) Set the threshold as $h = \mu + 3\sigma$, where μ and σ are the mean, and the standard deviation of $I_1(x,y) - I_2(x,y)$, respectively [21]. If $I_1(x,y;z_j) > h$ and $I_2(x,y;z_j) > h$, mark the block as an image area; otherwise, it is a speckle noise area. Get the noise matrix, $N_k(x,y;z_j)$, based on the following algorithm:

$$N_k(x,y;z_j) = \begin{cases} 0, & \text{if } I_1(x,y;z_j) \geq h \text{ and } I_2(x,y;z_j) \geq h \\ I_k(x,y;z_j), & \text{otherwise} \end{cases}, \quad (5)$$

where $k = 1$ or 2.
(4) Get the despeckling image, $I_{\mathrm{out}}(x,y;z_j)$, where

$$I_{\mathrm{out}}(x,y;z_j) = I_k(x,y;z_j) - N_k(x,y;z_j). \quad (6)$$

(5) Do CC labeling and remove the connected components that are too small. Here, we define the small area, s, satisfying $s < 0.1 s_{\max}$, where $s_{\max}$ is the maximum area in all of the connected components.

CC labeling is a common approach to extract an object in binary images, in which a unique label is assigned to each maximal connected region of foreground pixels [19,20]. The main process of this algorithm is as follows: first, zero is assigned to each pixel of background; then, a temporary label is assigned to each foreground pixel based on the values of its neighbors; finally, if a "conflict" is found, i.e., two foreground neighbors carrying different labels, then these pixels are registered as being equivalent and relabeled. The connected components whose areas are too small will be deleted in the very last steps, after which the object would be extracted.

The proposed method is demonstrated via simulation with an object containing two sections, as is shown in Fig. 3(a). Each section has a size of 1 mm × 1 mm, and is sampled to 512 × 512 pixels. The section distances are $z_1 = 9$ mm and $z_2 = 10$ mm, respectively. A laser source with wavelength equal to 632 nm is used in the simulation. The diameter of the collimated beam is $D = 40$ mm, and the focal length of lens 1 and lens 2 is $f = 75$ mm. The random phase mask encoded on pupil $p_2(x,y)$ can be realized by a liquid

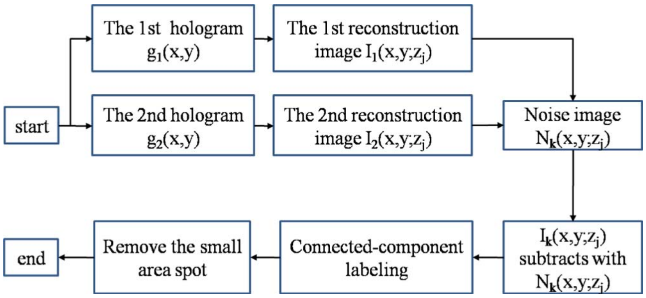

Fig. 2. Flow chart of the FDCC algorithm.

crystal on silicon (LCoS) transmissive spatial light modulator (SLM).

The reconstructed sectional images in a random phase encoded OSH system using a traditional method at $z = z_1, z_2$ are shown in Figs. 3(b) and 3(c), respectively. One can see that the reconstructed images suffer from large speckle-like defocus noise.

To eliminate this out-of-focus haze, we have implemented various methods for sectioning: (1) the averaging method; (2) the FD method, the algorithm of which contains steps (1)–(4) mentioned above; (3) the CC labeling method, the detail of which is illustrated in step (5) above; and (4) the proposed FDCC method. The results are shown in Fig. 4.

In the averaging method, 20 different section images obtained from 20 independent random phase masks are used. One can see from Figs. 4(a) and 4(b) that the speckle-like pattern has been suppressed by averaging to some extent; however, the signal-to-noise ratio (SNR) has not been improved greatly. Although better effect can be achieved by using more sectional images, the method is still quite time-consuming and inefficient.

In the FD method, two different sectional images are retrieved from two holograms for speckle reduction. The results are shown in Figs. 4(c) and 4(d). One can see from this figure that speckle-like patterns have been greatly eliminated, leaving only a few small spots. The noise spots can further be reduced by adjusting the threshold, h; however, it is hard to balance between eliminating the small spots and keeping the object.

The CC labeling, in which a single reconstructed sectional image is needed, also has been implemented. The results are shown in Figs. 4(e) and 4(f), with focused planes at z_1 and z_2, respectively. One can observe that the noise spots separated from the object have been eliminated perfectly; however, the ones that are close to the object image are retained and connected to it.

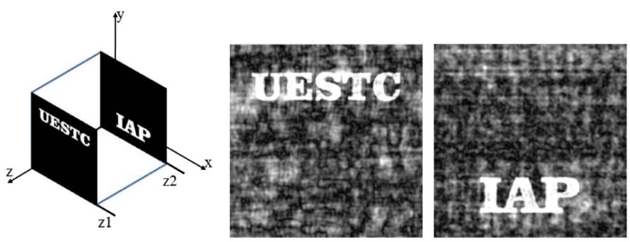

(a) (b) (c)

Fig. 3. (a) Two-section object. (b), (c) Sectioning using conventional method in a random phase encoded OSH system, with reconstruction distance at z_1 and z_2, respectively.

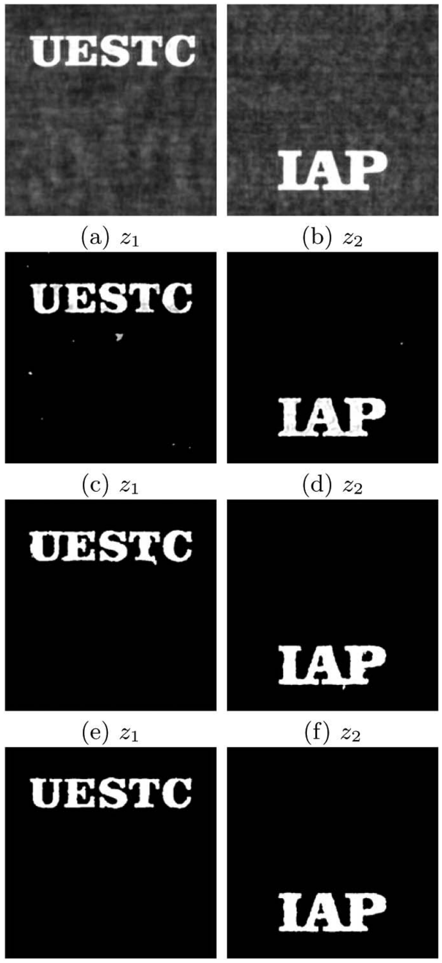

(a) z_1 (b) z_2 (c) z_1 (d) z_2 (e) z_1 (f) z_2 (g) z_1 (h) z_2

Fig. 4. Sectioning results using the average method [(a), (b)]; FD method [(c), (d)]; CC labeling method [(e), (f)]; and proposed FDCC method [(g), (h)].

The results based on the proposed FDCC method are shown in Figs. 4(h) and 4(g), in which the speckle-like patterns have been eliminated perfectly. One can see that the proposed FDCC method outperforms the other methods, and, therefore, is a highly promising sectioning approach which yields enhanced quality for further analysis. Less ambiguity of the sectional images after despeckling will enable more accurate applications, such as image segmentation.

To assess the quantitative performance of the four despeckling techniques mentioned above, we also analyze the SNR with different random phase masks. Table 1 lists the respective results, in which n denotes different random phase masks used in the evaluation. As expected, in all cases, the SNR shows improvement compared with the original image. One can also see that the proposed method outperforms the others with different random phase masks, which demonstrates the effectiveness of the proposed approach for speckle-like defocus noise reduction.

Table 1. SNR for Different Methods (dB)

Method \ n	1	2	3	4
Original	25.9	27.4	26.3	28.5
Averaging	28.3	29.4	29.1	28.7
Frame Difference	44.6	44.9	43.8	42.6
Connected Component	43.8	41.2	43.4	41.8
FDCC	44.9	45.1	43.9	44.3

In conclusion, we presented for the first time, to the best of our knowledge, a speckle reduction based on a combined FDCC method in a random phase encoded OSH system. The sectioning image quality has been improved with enhanced visibility. It is demonstrated that, by combining the frame difference and the connected component methods, a trade-off between speckle reduction and edge preservation can be achieved.

Funding. National Natural Science Foundation of China (NSFC) (61107018, 61361166008); Research Grants Council, University Grants Committee, Hong Kong (RGC, UGC) (HKU 7131/12E, N-HKU714/13).

REFERENCES

1. J. Swoger, M. Martínez-Corral, J. Huisken, and E. H. K. Stelzer, J. Opt. Soc. Am. A **19**, 1910 (2002).
2. G. Indebetouw and W. Zhong, J. Opt. Soc. Am. A **23**, 1699 (2006).
3. B. W. Schilling and G. C. Templeton, Appl. Opt. **40**, 5474 (2001).
4. T. Kim, T.-C. Poon, and G. Indebetouw, Opt. Eng. **41**, 1331 (2002).
5. T.-C. Poon, T. Kim, and K. Doh, Appl. Opt. **42**, 6496 (2003).
6. H. Di, K. Zheng, X. Zhang, E. Y. Lam, T. Kim, Y. S. Kim, T.-C. Poon, and C. Zhou, Appl. Opt. **51**, 1000 (2012).
7. T.-C. Poon, *Optical Scanning Holography with MATLAB* (Springer, 2007).
8. E. Y. Lam, X. Zhang, H. Vo, T.-C. Poon, and G. Indebetouw, Appl. Opt. **48**, H113 (2009).
9. X. Zhang, E. Y. Lam, and T.-C. Poon, Opt. Express **16**, 17215 (2008).
10. T. Kim, Appl. Opt. **45**, 872 (2006).
11. H. Kim, S.-W. Min, B. Lee, and T.-C. Poon, Appl. Opt. **47**, D164 (2008).
12. J. Ke, T.-C. Poon, and E. Y. Lam, Appl. Opt. **50**, H285 (2011).
13. H. Ou, T.-C. Poon, K. K. Wong, and E. Y. Lam, Appl. Opt. **52**, 3079 (2013).
14. H. Ou, T.-C. Poon, K. K. Y. Wong, and E. Y. Lam, Photon. Res. **2**, 64 (2014).
15. Z. Xin, K. Dobson, Y. Shinoda, and T.-C. Poon, Opt. Lett. **35**, 2934 (2010).
16. P. Refregier and B. Javidi, Opt. Lett. **20**, 767 (1995).
17. C. Zhan, X. Duan, S. Xu, Z. Song, and M. Luo, *Fourth International Conference on Image and Graphics*, (IEEE, 2007), pp. 519–523.
18. H. Chu, S. Ye, Q. Guo, and X. Liu, *IEEE International Conference on Automation and Logistics*, (IEEE, 2007), pp. 51–55.
19. H. Lifeng, C. Yuyan, and S. Kenji, IEEE Trans. Pattern Anal. Mach. Intell. **20**, 2122 (2011).
20. L. He and Y. Chao, IEEE Trans. Image Process. **24**, 2725 (2015).
21. I. Haritaoglu, D. Harwood, and L. S. Davis, IEEE Trans. Pattern Anal. Mach. Intell. **22**, 809 (2000).